Hindawi Publishing Corporation
Mathematical Problems in Engineering
Volume 2014, Article ID 237234, 14 pages
http://dx.doi.org/10.1155/2014/237234

Research Article

A Transformation Method for Solving Conservative Nonlinear Two-Degree-of-Freedom Systems

Alex Elías-Zúñiga, Daniel Olvera Trejo, Inés Ferrer Real, and Oscar Martínez-Romero

Departamento de Ingeniería Mecánica, Tecnológico de Monterrey, Campus Monterrey, E. Garza Sada 2501 Sur, 64849 Monterrey, N.L., Mexico

Correspondence should be addressed to Alex Elías-Zúñiga; aelias@itesm.mx

Received 9 October 2013; Revised 30 January 2014; Accepted 16 March 2014; Published 7 May 2014

Academic Editor: Michael J. Brennan

A nonlinear transformation approach based on a cubication method is developed to obtain the equivalent representation form of conservative two-degree-of-freedom nonlinear oscillators. It is shown that this procedure leads to equivalent nonlinear equations that describe well the numerical integration solutions of the original equations of motion.

1. Introduction

Recently, we have introduced in [1, 2] a procedure that transforms the original equation of motion of single degree of freedom systems, having nonlinear restoring forces, into nonlinear ordinary differential equations of the Duffing type. Furthermore, this procedure has been used in conjunction with the Chebyshev polynomials to derive the equivalent representation form of nonlinear system with dissipative and sinusoidal driving forces [2] in which the numerical comparisons between the equivalent and the original equations of motion demonstrate the effectiveness of this method in predicting the corresponding system dynamics response. Motivated by these results, we herein expand the application of this technique to obtain the equivalent representation form of two-degree-of-freedom homogeneous, undamped, and ordinary differential equations of the form

$$\begin{Bmatrix} m_1 & 0 \\ 0 & m_2 \end{Bmatrix} \begin{bmatrix} \ddot{x}_1 \\ \ddot{x}_2 \end{bmatrix} + \begin{Bmatrix} k_{11} & k_{12} \\ k_{21} & k_{22} \end{Bmatrix} \begin{bmatrix} x_1 \\ x_2 \end{bmatrix} + \begin{Bmatrix} f_1(x_1, x_2) \\ f_2(x_1, x_2) \end{Bmatrix} = 0 \quad (1)$$

that models the dynamics response of systems that arise in physics and engineering applications [3–6], where m_1 and m_2 are the masses of the system, k_{11}, k_{12}, k_{21}, and k_{22} are stiffness parameters, $f_1(x_1, x_2)$ and $f_2(x_1, x_2)$ are nonlinear restoring forces, and $x_1(0) = x_{10}$, $\dot{x}_1(0) = \dot{x}_{10}$, $x_2(0) = x_{20}$, and $\dot{x}_2(0) = \dot{x}_{20}$ are the system initial conditions.

The method is based on replacing first the system restoring forces by polynomial expressions and, then, we use a transformation technique to replace the resulting equations by two uncoupled nonlinear differential equations of the Duffing type whose solutions are based on Jacobi elliptic functions. It is shown that the appropriate derivation of one of these solutions can improve the numerical estimates of the equivalent equations of motion even at larger and feasible nonlinear parameter
values.

2. A Nonlinear Transformation Approach

The equivalent representation form of (1) is obtained by replacing it by two uncoupled, nonlinear ordinary differential equations of the Duffing type by following an approach similar to the one described in [1], This procedure yields

$$\ddot{x}_1 + a_1 x_1 + a_2 x_1^3 = 0; \qquad \ddot{x}_2 + a_3 x_2 + a_4 x_2^3 = 0. \quad (2)$$

Here we assume that the coefficients a_i are determined by the following expressions:

$$\frac{\partial F_1(a_1,a_2)}{\partial a_1}=0,\qquad \frac{\partial F_1(a_1,a_2)}{\partial a_2}=0,$$
$$\frac{\partial F_2(a_3,a_4)}{\partial a_3}=0,\qquad \frac{\partial F_2(a_3,a_4)}{\partial a_4}=0, \tag{3}$$

where

$$F_1(a_1,a_2)=\int_0^{u_2}\int_0^{u_1}\left(\frac{k_{11}x_1+k_{12}x_2+f_1(x_1,x_2)}{m_1}-a_1x_1-a_2x_1^3\right)^2dx_1dx_2\longrightarrow\min, \tag{4}$$

$$F_2(a_3,a_4)=\int_0^{u_4}\int_0^{u_3}\left(\frac{k_{21}x_1+k_{22}x_2+f_2(x_1,x_2)}{m_2}-a_3x_2-a_4x_2^3\right)^2dx_2dx_1\longrightarrow\min \tag{5}$$

and the values of u_i are fitted to satisfy (4) and (5) [7]. Notice, in this case, that the system (2) can be solved in closed form by using Jacobi elliptic functions. This yields [8]

$$x_1=x_{10}cn\left(\omega_1t,\kappa_1^2\right),\qquad \omega_1=\sqrt{a_1+a_2x_{10}^2},$$
$$\kappa_1^2=\frac{a_2x_{10}^2}{2\omega_1^2},$$
$$x_2=x_{20}cn\left(\omega_2t,\kappa_2^2\right),\qquad \omega_2=\sqrt{a_3+a_4x_{20}^2},$$
$$\kappa_2^2=\frac{a_3x_{20}^2}{2\omega_2^2}. \tag{6}$$

However, an alternative approach to find the equivalent representation form of (1) can be derived if we use the form $(2)_1$ or $(2)_2$ and then substitute its exact solution into the remaining equation in (1). In this case, the influence of the nonlinear effects of x_1 or x_2 into the system dynamics response will be taken into account by the resulting coupled equation of motion whose approximate solution could be based on the usage of Jacobi elliptic functions.

Other equivalent representation forms of (1) are possible since these depend on the polynomial order use to write the equivalent form of the system restoring forces [9–11]. For instance, let us suppose that the nonlinear conservative forces of (1) are of the cubic type and rewrite (1) in its canonical representation form [12]:

$$\begin{Bmatrix}\ddot{u}_1\\ \ddot{u}_2\end{Bmatrix}+\begin{Bmatrix}\omega_{n1}^2 & 0\\ 0 & \omega_{n2}^2\end{Bmatrix}\begin{bmatrix}u_1\\ u_2\end{bmatrix}+\varepsilon\begin{Bmatrix}\varphi_1u_1^3+\varphi_2u_1^2u_2+\varphi_3u_1u_2^2+\varphi_4u_2^3\\ \varphi_5u_1^3+\varphi_6u_1^2u_2+\varphi_7u_1u_2^2+\varphi_8u_2^3\end{Bmatrix}=0, \tag{7}$$

with initial conditions given as $u_1(0)=u_{10}$, $\dot{u}_1(0)=\dot{u}_{10}$, $u_2(0)=u_{20}$, and $\dot{u}_2(0)=\dot{u}_{20}$. Here the dots denote the time derivative, u_1 and u_2 are known as the system normal coordinates, ε is a nonlinear parameter, and ω_{n1}, ω_{n2}, and φ_1 through φ_8 are corresponding system parameters that are defined in accordance with the physics of the system. Now, let us replace (7) by their corresponding equivalent equations of motion of the Duffing type which are valid for the complete range of oscillation amplitudes [1], by using the relations

$$F_1(b_1,b_2)=\int_0^{\nu_2}\int_0^{\nu_1}\left(\omega_{n1}^2u_1+\varepsilon\left(\varphi_1u_1^3+\varphi_2u_1^2u_2+\varphi_3u_1u_2^2+\varphi_4u_2^3\right)-b_1u_1-b_2u_1^3\right)^2du_1du_2\longrightarrow\min,$$
$$F_2(b_3,b_4)=\int_0^{\nu_{11}}\int_0^{\nu_{22}}\left(\omega_{n2}^2u_2+\varepsilon\left(\varphi_5u_1^3+\varphi_6u_1^2u_2+\varphi_7u_1u_2^2+\varphi_8u_2^3\right)-b_3u_2-b_4u_2^3\right)^2du_2du_1\longrightarrow\min, \tag{8}$$

where ν_1, ν_2, ν_{11}, and ν_{22} are fitted constants that satisfy (8), and the parameters b_i are determined by solving the equations

$$\frac{\partial F_1(b_1,b_2)}{\partial b_1}=0,\qquad \frac{\partial F_1(b_1,b_2)}{\partial b_2}=0,$$
$$\frac{\partial F_2(b_3,b_4)}{\partial b_3}=0,\qquad \frac{\partial F_2(b_3,b_4)}{\partial b_4}=0. \tag{9}$$

This yields

$$b_1=-\frac{-30\varphi_2\nu_1\nu_2-64\varphi_3\nu_1\nu_2^2-135\varphi_4\nu_2^3-192\nu_1\omega_{n1}^2}{192\nu_1},$$
$$b_2=-\frac{-192\varphi_1\nu_1^3-70\varphi_2\nu_1^2\nu_2+105\varphi_4\nu_2^3}{192\nu_1^3},$$
$$b_3=-\frac{-135\varphi_5\nu_{11}^3-64\varphi_6\nu_{11}^2\nu_{22}-30\varphi_7\nu_{11}\nu_{22}^2-192\nu_{22}\omega_{n2}^2}{192\nu_{22}},$$
$$b_4=-\frac{-105\varphi_5\nu_{11}^3-70\varphi_7\nu_{11}\nu_{22}^2-192\varphi_8\nu_{22}^3}{192\nu_{22}^3}. \tag{10}$$

Then, (7) can be rewritten in equivalent form as

$$\ddot{u}_1+b_1u_1+b_2u_1^3=0,\qquad \ddot{u}_2+b_3u_2+b_4u_2^3=0, \tag{11}$$

whose exact solutions are similar to those given by (6).

We shall next explore the applicability of the nonlinear transformation method in obtaining the equivalent representation form of (1) and, then, we will compare the numerical integration solutions of five dynamics systems, having nonlinear restoring forces with rational or irrational terms, with respect to their equivalent representation forms [13–20]. First, let us consider the case for which the restoring forces are of the cubic type.

Table 1: RMSE values computed from the equivalent representation forms of (13) with $u_1 = 1.55$, $u_2 = 1.5$, $u_3 = 1.25$, and $u_4 = 1.6$. Here $b_{11} = (k_1 + k_2)/m_1$, $b_{12} = b_{21} = -k_2 x_{20}/(m_1 x_{10})$, $b_{22} = 2k_2/m_2$, and $d_1 = \varepsilon x_{10}^2/m_1$.

ε	$\ddot{y}_1 + a_1 y_1 + a_2 y_1^3 = 0$, $\ddot{y}_2 + a_3 y_2 + a_4 y_2^3 = 0$.		$\ddot{y}_1 + a_1 y_1 + a_2 y_1^3 = 0$, $\ddot{y}_2 + b_{21} y_1 + b_{22} y_2 = 0$.		$\ddot{y}_2 + a_3 y_2 + a_4 y_2^3 = 0$, $\ddot{y}_1 + b_{11} y_1 + b_{12} y_2 + d_1 y_1^3 = 0$.	
	RMSE $y_1(x)$	RMSE $y_2(x)$	RMSE $y_1(x)$	RMSE $y_2(x)$	RMSE $y_1(x)$	RMSE $y_2(x)$
0.01	0.2992	0.9138	0.2992	0.3062	1.1924	0.9138
0.25	0.3248	0.8863	0.3248	0.4004	0.1797	0.8863
0.75	0.1511	0.8222	0.1511	0.2873	0.2167	0.8222
1.50	0.0398	0.8373	0.0398	0.1989	0.1902	0.8373
5	0.1488	0.9068	0.1488	0.0818	0.0930	0.9068
20	0.1179	0.9490	0.1179	0.0233	0.0082	0.9490
100	0.0697	0.9635	0.0697	0.0047	0.0011	0.9635

2.1. Example 1: A Cubic Nonlinear System. Let us consider the conservative system built with a nonlinear spring of the cubic type. The corresponding equations of motion are given as [13]

$$\begin{Bmatrix} m_1 & 0 \\ 0 & m_2 \end{Bmatrix} \begin{bmatrix} \ddot{x}_1 \\ \ddot{x}_2 \end{bmatrix} + \begin{Bmatrix} k_1 + k_2 & -k_2 \\ -k_2 & 2k_2 \end{Bmatrix} \begin{bmatrix} x_1 \\ x_2 \end{bmatrix} + \begin{Bmatrix} \varepsilon x_1^3 \\ 0 \end{Bmatrix} = 0, \tag{12}$$

with initial conditions $x_1(0) = x_{10}$, $\dot{x}_1(0) = 0$, $x_2(0) = x_{20}$, and $\dot{x}_2(0) = 0$. If we introduce the transformations $y_1 = x_1/x_{10}$ and $y_2 = x_2/x_{20}$ so that $y_1(0) = 1$, $\dot{y}_1(0) = 0$, $y_2(0) = 1$, $\dot{y}_2(0) = 0$, thus (12) can be written in normalized form as

$$\begin{Bmatrix} 1 & 0 \\ 0 & 1 \end{Bmatrix} \begin{bmatrix} \ddot{y}_1 \\ \ddot{y}_2 \end{bmatrix} + \begin{Bmatrix} \dfrac{(k_1 + k_2)}{m_1} & -\dfrac{k_2 x_{20}}{(m_1 x_{10})} \\ -\dfrac{k_2 x_{10}}{(m_2 x_{20})} & \dfrac{2k_2}{m_2} \end{Bmatrix} \begin{bmatrix} y_1 \\ y_2 \end{bmatrix} + \begin{Bmatrix} \dfrac{\varepsilon x_{10}^2 y_1^3}{m_1} \\ 0 \end{Bmatrix} = 0. \tag{13}$$

If we use our proposed nonlinear transformation approach then the equivalent representation form of (13) is given as

$$\ddot{y}_1 + a_1 y_1 + a_2 y_1^3 = 0; \qquad \ddot{y}_2 + a_3 y_2 + a_4 y_2^3 = 0, \tag{14}$$

where the a_i, determined from (4) and (5), are given as

$$\begin{aligned} a_1 &= -\frac{-32k_1 u_1 x_{10} - 32k_2 u_1 x_{10} + 45k_2 u_2 x_{20}}{32 m_1 u_1 x_{10}}, \\ a_2 &= -\frac{-32\varepsilon u_1^3 x_{10}^3 - 35k_2 u_2 x_{20}}{32 m_1 u_1^3 x_{10}}, \\ a_3 &= -\frac{45k_2 u_{11} x_{10} - 32k_2 u_{22} x_{20}}{32 m_2 u_{22} x_{20}}, \\ a_4 &= \frac{35k_2 u_{11} x_{10}}{32 m_2 u_{22}^3 x_{20}}, \end{aligned} \tag{15}$$

and u_1, u_2, u_{11}, and u_{22} are the corresponding fitting parameters described earlier.

To apply our nonlinear transformation approach to the canonical representation form of (13), we first use the following linear coordinate transformation [12]:

$$\begin{bmatrix} x_1 \\ x_2 \end{bmatrix} = \begin{Bmatrix} R_1 & R_2 \\ R_1 f_1 & R_2 f_2 \end{Bmatrix} \begin{bmatrix} u_1 \\ u_2 \end{bmatrix}, \tag{16}$$

which yields the canonical form (7). Here, the system parameters of (7) are described by the relations

$$\begin{aligned} \omega_{n1}^2 &= \frac{1}{2m_1}\left[(k_1 + 3k_2) - \sqrt{k_1^2 - 2k_1 k_2 + 5k_2^2}\right], \\ \omega_{n2}^2 &= \frac{1}{2m_1}\left[(k_1 + 3k_2) + \sqrt{k_1^2 - 2k_1 k_2 + 5k_2^2}\right], \\ \varphi_1 &\equiv -\varepsilon R_1^4 x_{10}^2, \qquad \varphi_2 \equiv -3\varepsilon R_1^3 R_2 x_{10} x_{20}, \\ \varphi_3 &\equiv -3\varepsilon R_1^2 R_2^2 x_{20}^2, \qquad \varphi_4 \equiv -\frac{\varepsilon R_1 R_2^3 x_{20}^3}{x_{10}}, \\ \varphi_5 &\equiv -\frac{\varepsilon R_1^3 R_2 x_{10}^3}{x_{20}}, \qquad \varphi_6 \equiv -3\varepsilon R_1^2 R_2^2 x_{10}^2, \\ \varphi_7 &\equiv -3\varepsilon R_1 R_2^3 x_{10} x_{20}, \qquad \varphi_8 \equiv -\varepsilon R_2^4 x_{20}^2, \\ f_1 &\equiv \frac{k_1 + k_2 - m_1 \omega_{n1}^2}{k_2}, \qquad f_2 \equiv \frac{k_1 + k_2 - m_1 \omega_{n2}^2}{k_2}, \\ R_1^2 &\equiv \frac{1}{m_1 (1 + f_1^2)}, \qquad R_2^2 \equiv \frac{1}{m_1 (1 + f_2^2)}. \end{aligned} \tag{17}$$

Thus, the approximate solutions of (13), by considering their canonical representation form, are given by expressions similar to those of (6).

Tables 1 and 2 show the root-mean-square error (RMSE) values computed by comparing the numerical integration solutions of the original equations of motion (13), with respect to numerical results computed from their derived equivalent representation forms by considering the initial conditions values of $x_1(0) = 2$, $\dot{x}_1(0) = 0$, $x_2(0) = -1$, and $\dot{x}_2(0) = 0$, the parameter values of $m_1 = m_2 = 1$, $k_1 = 3$, and $k_2 = 1$, and different values of ε. In the second and third

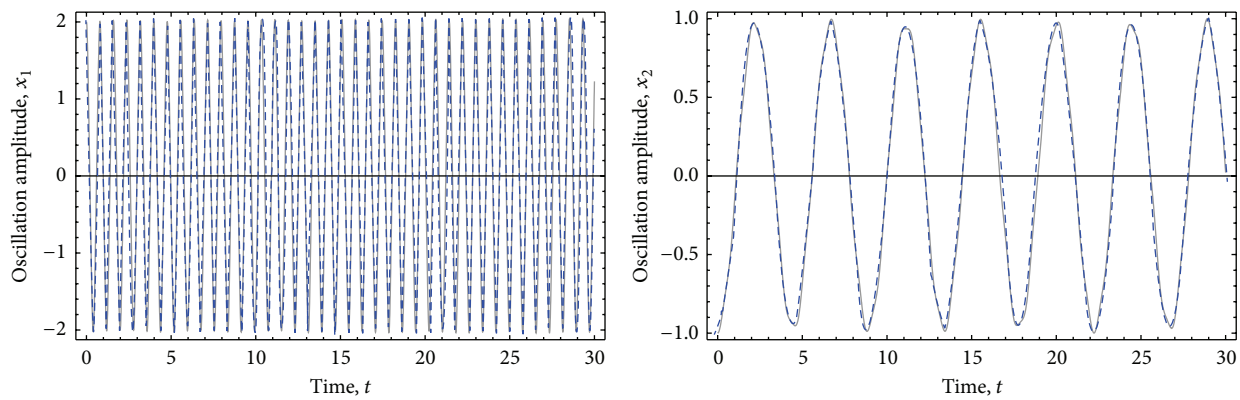

(a) (b)

Figure 1: Amplitude-time response curves computed from the numerical integration solutions of (13) and those provided by substituting $(14)_1$ into $(13)_2$. The parameter values used to obtain these plots were $m_1 = m_2 = 1$, $k_1 = 3$, $k_2 = 1$, and $\varepsilon = 20$, with $x_1(0) = 2$, $\dot{x}_1(0) = 0$, $x_2(0) = -1$, and $\dot{x}_2(0) = 0$, and $u_1 = 1.55$, $u_2 = 1.5$, $u_3 = 1.25$, and $u_4 = 1.6$. Here, the gray solid lines describe the numerical integration solutions of (13), while the blue dashed lines represent the numerical solutions obtained from the derived equivalent nonlinear equations of motion.

Table 2: RMSE values computed by considering the canonical representation form of (13) with $\nu_1 = -9$, $\nu_2 = -0.215$, $\nu_{11} = -2.325$, and $\nu_{22} = -8.5$.

ε	$\ddot{u}_1 + b_1u_1 + b_2u_1^3 = 0$, $\ddot{u}_2 + b_3u_2 + b_4u_2^3 = 0$.		$\ddot{u}_1 + b_1u_1 + b_2u_1^3 = 0$, $\ddot{u}_2 + \omega_{n2}^2u_2 + \varepsilon\{\varphi_5u_1^3 + \varphi_6u_1^2u_2 + \varphi_7u_1u_2^2 + \varphi_8u_2^3\} = 0$.		$\ddot{u}_2 + b_3u_2 + b_4u_2^3 = 0$, $\ddot{u}_1+\omega_{n1}^2u_1+\varepsilon\{\varphi_1u_1^3+\varphi_2u_1^2u_2+\varphi_3u_1u_2^2+\varphi_4u_2^3\} = 0$.	
	RMSE $u_1(x)$	RMSE $u_2(x)$	RMSE $u_1(x)$	RMSE $u_2(x)$	RMSE $u_1(x)$	RMSE $u_2(x)$
0.01	0.06010	0.0277	0.0044	0.0109	0.0606	0.0248
0.25	1.5351	0.6069	0.3611	0.2661	1.5824	0.4956
0.75	2.0910	0.8049	1.3988	0.6512	2.2351	0.7348
1.50	2.1222	0.8349	2.1151	0.8220	2.5577	1.1983
5	1.9552	0.8733	1.8608	0.8739	3.1331	8.8874
20	1.9116	0.9044	1.9889	0.9090	3.1549	8.7513
100	1.9495	0.9136	1.9704	0.9191	3.4887	8.1949

columns of Table 1 are tabulated the RMSE values computed by using the equivalent representation forms of (13) given by (14), while the fourth and the fifth columns provide the RMSE values obtained by substituting $(14)_1$ into $(13)_2$. The sixth and the seventh columns of Table 1 contain the RMSE values computed by substituting $(14)_2$ into $(13)_1$. As we can see from Table 1, the lowest RMSE values are tabulated in the fifth and the sixth columns which implies that the most accurate solutions of (13) are obtained when the equivalent representation form $(14)_1$ is used to derive the approximate solution of x_2. Also notice from Table 1, that the computed values of the RMSE become smaller for increasing values of the nonlinear parameter ε which shows that our solution procedure can be used to obtain solutions that follow the numerical integration solutions of the original equations of motion even at larger values of ε. For illustrative purposes, we have plotted in Figure 1 the amplitude-time response curves obtained from (13), and those provided by substituting $(14)_1$ into $(13)_2$. We have selected the value of $\varepsilon = 20$ which provides a highly nonlinear dynamic system response. Notice from Figure 1 that both solutions are almost the same. In fact, the RMSE values do not exceed 0.1179, for x_1, and 0.0233, for x_2. In Figure 1, the gray solid lines describe the numerical integration solutions of (13), while the blue dashed lines represent the numerical solutions obtained from our derived equivalent nonlinear equations of motion.

Table 2 shows the RMSE values obtained by using the canonical representation form of (13). One can notice from Table 2 that the smallest RMSE values were computed at decreasing values of the nonlinear parameter ε when the equivalent form $(11)_1$ was substituted into $(7)_2$ (the fifth and the sixth columns). Also, one can notice that when $\varepsilon = 0$, (7) describes the oscillatory behavior of the resulting linear dynamics system; however, this is not the case when we use the equivalent representation form of (13) given by (14) because the terms a_2 and a_4 are different from zero. This situation increases the RMSE errors as listed in Table 1. In an attempt to further quantify the accuracy of our proposed

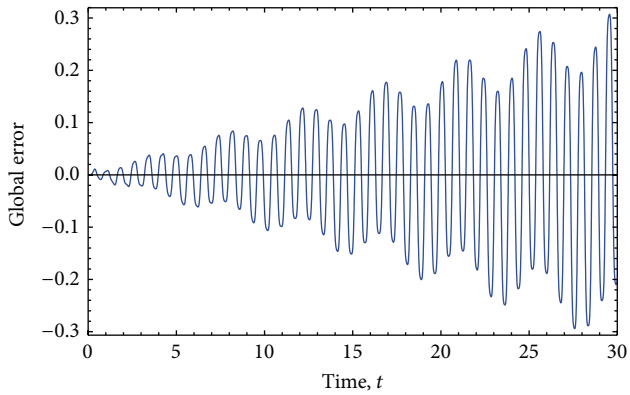

Figure 2: Global error behavior.

procedure, we next introduce the global error estimation based on a technique similar to the ones developed in [14–16] in which the system global error, GE, can be determined from the following expression:

$$\mathrm{GE} = \left(y_1(t) - p_1(t)\right) + \left(y_2(t) - p_2(t)\right), \tag{18}$$

where y_1 and y_2 represent the values obtained by numerically integrating the equivalent equations of motion and p_1 and p_2 are the numerical values computed by using the original system equations of motion. Figure 2 displays the global error curve plotted versus time by considering the numerical integration solutions of both, the resulting equation obtained by substituting $(14)_1$ into $(13)_2$ and the original equations of motion (13). One can notice from Figure 2, that the global error tends to grow linearly at increasing time values, as predicted by Calvo and Hairer in [14].

To further assess the accuracy of our proposed nonlinearization method, we will next examine a hyperelastic shear suspension system.

2.2. Example 2: Hyperelastic Shear Suspension System. Here the equations of motion of a linear absorber attached to a rigid body that is supported symmetrically by incompressible, homogeneous, and isotropic hyperelastic shear blocks are given as

$$\begin{Bmatrix} 1 & 0 \\ 0 & \beta \end{Bmatrix} \begin{bmatrix} \ddot{\sigma} \\ \ddot{z} \end{bmatrix} + \begin{Bmatrix} 1 & -\alpha_2^2 \\ -\alpha_2^2 & \alpha_2^2 \end{Bmatrix} \begin{bmatrix} \sigma \\ z \end{bmatrix} - \begin{Bmatrix} \varepsilon b_1 \sigma^3 \\ 0 \end{Bmatrix} = 0, \tag{19}$$

with initial conditions given as $\sigma(0) = \sigma_{10}$, $\dot{\sigma}(0) = 0$, $z(0) = z_{10}$, and $\dot{z}(0) = 0$. Here σ and z denote, respectively, the simple shear deformation of the load and the motion of the linear absorber system, ε describes the nonlinear material response effects, r_2 is a tuning system parameter, and β, α_2, and b_1 are defined as

$$\beta = \frac{m}{M}, \qquad b_1 = \alpha_2^2 - 1, \qquad \alpha_2^2 = \frac{\beta r_2^2}{\beta r_2^2 + 1}. \tag{20}$$

The details of the derivation of the equations of motion given by (19) are provided in [2]. Next, we set $y_1 = \sigma/\sigma_{10}$ and $y_2 = z/z_{10}$ and rewrite (12) in its normalized form

$$\begin{Bmatrix} 1 & 0 \\ 0 & 1 \end{Bmatrix} \begin{bmatrix} \ddot{y}_1 \\ \ddot{y}_2 \end{bmatrix} + \begin{Bmatrix} 1 & -\dfrac{\alpha_2^2 z_{10}}{\sigma_{10}} \\ -\dfrac{\alpha_2^2 \sigma_{10}}{(\beta z_{10})} & \dfrac{\alpha_2^2}{\beta} \end{Bmatrix} \begin{bmatrix} y_1 \\ y_2 \end{bmatrix} - \begin{Bmatrix} \varepsilon \sigma_{10}^2 y_1^3 \\ 0 \end{Bmatrix} = 0 \tag{21}$$

with $y_1(0) = 1$, $\dot{y}_1(0) = 0$, $y_2(0) = 1$, and $\dot{y}_2(0) = 0$. Notice that the canonical representation form of (21) can be obtained by using the transformation (16); this yields exactly (7), where the system parameters are given by the following relations:

$$\begin{gathered}
\omega_{n1}^2 = \frac{1}{2}\left[\left(\frac{\alpha_2^2}{\beta} + 1\right) - \sqrt{\left(\frac{\alpha_2^2}{\beta} + 1\right)^2 + \frac{4\alpha_2^2 b_1}{\beta}}\right], \\
\omega_{n2}^2 = \frac{1}{2}\left[\left(\frac{\alpha_2^2}{\beta} + 1\right) + \sqrt{\left(\frac{\alpha_2^2}{\beta} + 1\right)^2 + \frac{4\alpha_2^2 b_1}{\beta}}\right], \\
\varphi_1 \equiv -b_1 \varepsilon R_1^4 \sigma_{10}^2, \qquad \varphi_2 \equiv -3 b_1 \varepsilon R_1^3 R_2 \sigma_{10} z_{20}, \\
\varphi_3 \equiv -3 b_1 \varepsilon R_1^2 R_2^2 z_{20}^2, \qquad \varphi_4 \equiv -\frac{b_1 \varepsilon R_1 R_2^3 z_{20}^3}{\sigma_{10}}, \\
\varphi_5 \equiv -\frac{b_1 \varepsilon R_1^3 R_2 \sigma_{10}^3}{z_{20}}, \qquad \varphi_6 \equiv -3 b_1 \varepsilon R_1^2 R_2^2 \sigma_{10}^2, \\
\varphi_7 \equiv -3 b_1 \varepsilon R_1 R_2^3 \sigma_{10} z_{20}, \qquad \varphi_8 \equiv -b_1 \varepsilon R_2^4 z_{20}^2, \\
f_1 \equiv \frac{1 - \omega_{n1}^2}{\alpha_2^2}, \qquad f_2 \equiv \frac{1 - \omega_{n2}^2}{\alpha_2^2}, \\
R_1^2 \equiv \frac{1}{(1 + f_1^2 \beta)}, \qquad R_2^2 \equiv \frac{1}{(1 + f_2^2 \beta)}.
\end{gathered} \tag{22}$$

Since $(21)_2$ is only coupled with y_1 through the linear term $-\alpha_2^2 \sigma_{10}/(\beta z_{10}) y_1$, we slightly modify our procedure and assume that the equivalent representation form of (21) is given as

$$\ddot{y}_1 + a_1 y_1 + a_2 y_1^3 = 0; \qquad \ddot{y}_2 + a_3 y_2 = 0, \tag{23}$$

Table 3: RMSE values computed from the equivalent representation forms of (21) with $u_1 = -0.4$, $u_2 = 0.1$, $u_3 = -0.01$, and $u_4 = -0.315$. Here $b_{11} = 1$, $b_{12} = b_{21} = -\alpha_2^2\sigma_{10}/(\beta z_{10})$, $b_{22} = \alpha_2^2/\beta$, and $d_1 = -\varepsilon\sigma_{10}^2$.

ε	$\ddot{y}_1 + a_1 y_1 + a_2 y_1^3 = 0$, $\ddot{y}_2 + a_3 y_2 = 0$.		$\ddot{y}_1 + a_1 y_1 + a_2 y_1^3 = 0$, $\ddot{y}_2 + b_{21} y_1 + b_{22} y_2 = 0$.		$\ddot{y}_2 + a_3 y_2 = 0$, $\ddot{y}_1 + b_{11} y_1 + b_{12} y_2 + d_1 y_1^3 = 0$.	
	RMSE $y_1(x)$	RMSE $y_2(x)$	RMSE $y_1(x)$	RMSE $y_2(x)$	RMSE $y_1(x)$	RMSE $y_2(x)$
0.01	0.9448	1.3409	0.9448	2.3366	1.7724	1.3409
0.25	0.5880	1.2351	0.5880	1.1768	0.7684	1.2351
0.75	0.1609	1.0394	0.1609	0.1774	0.3309	1.0394
1.5	0.2402	0.7685	0.2402	0.2079	0.3157	0.7685
5	0.3637	0.4461	0.3637	0.1376	0.0910	0.4461
20	0.2489	0.3267	0.2489	0.0414	0.0125	0.3267
100	0.1226	0.2995	0.1226	0.0083	0.0011	0.2995

Table 4: RMSE values computed by considering the canonical representation form of (21) with $\nu_1 = 0.85$, $\nu_2 = 0.45$, $\nu_{11} = -0.01$, and $\nu_{22} = 0.1$.

ε	$\ddot{u}_1 + b_1 u_1 + b_2 u_1^3 = 0$, $\ddot{u}_2 + b_3 u_2 + b_4 u_2^3 = 0$.		$\ddot{u}_1 + b_1 u_1 + b_2 u_1^3 = 0$, $\ddot{u}_2 + \omega_{n2}^2 u_2 + \varepsilon\{\varphi_5 u_1^3 + \varphi_6 u_1^2 u_2 + \varphi_7 u_1 u_2^2 + \varphi_8 u_2^3\} = 0$.		$\ddot{u}_2 + b_3 u_2 + b_4 u_2^3 = 0$, $\ddot{u}_1 + \omega_{n1}^2 u_1 + \varepsilon\{\varphi_1 u_1^3 + \varphi_2 u_1^2 u_2 + \varphi_3 u_1 u_2^2 + \varphi_4 u_2^3\} = 0$.	
	RMSE $u_1(x)$	RMSE $u_2(x)$	RMSE $u_1(x)$	RMSE $u_2(x)$	RMSE $u_1(x)$	RMSE $u_2(x)$
0.01	0.0077	0.0168	0.0066	0.0174	0.0028	0.0050
0.25	0.1953	0.3769	0.1325	0.3596	0.1516	0.2393
0.75	0.8844	1.2761	0.7365	1.1609	0.9850	0.9016
1	1.0156	1.3704	0.9953	1.4230	1.4544	3.8230
1.5	0.8727	1.1634	0.9922	1.3683	1.5028	4.3001
5	0.9301	1.2149	0.9678	1.4201	0.8801	4.0894
20	0.9010	1.2577	0.9729	1.5285	1.2238	3.8974
100	0.9282	1.270	1.0162	1.5621	1.2479	3.8438

where the parameters a_i, computed from (4), are given as

$$a_1 = -\frac{-32u_1\sigma_{10} + 45\alpha_2^2 u_2 z_{10}}{32u_1\sigma_{10}},$$

$$a_2 = -\frac{-32b_1\varepsilon u_1^3\sigma_{10}^3 - 35\alpha_2^2 u_2 z_{10}}{32u_1^3\sigma_{10}}, \tag{24}$$

$$a_3 = \frac{-\alpha_2^2 u_{11}\sigma_{10} + \alpha_2^2 u_{22} z_{10}}{\beta u_{22} z_{10}},$$

and u_1, u_2, u_{11}, and u_{22} are the corresponding fitting parameters. The assumption that $(21)_2$ can be transformed into a linear equation of the form $(23)_2$ is based on the fact that in $(21)_2$, there is not $y_2(t)$ terms of the cubic type.

Next, if the canonical representation form of (21) is considered, their approximate solutions, that can be obtained from (7), are given by (6). Tables 3 and 4 show the RMSE values computed from the numerical integration solutions of (21) and from the derived equivalent representation forms. Here, we have used as initial conditions the values of $\sigma_{10}(0) = 1$, $\dot{\sigma}(0) = 0$, $z_{10}(0) = -1$, and $\dot{z}(0) = 0$, with $\beta = 1/5$ and $r_2 = 1$. One can notice from Table 3 that the lowest RMSE values are tabulated in the fifth and the sixth columns at values of $\varepsilon > 0.25$. In fact, as the value of ε tends to increase, the RMSE values tend to decrease. Figure 3 shows the amplitude-time response curves computed by substituting $(23)_1$ into $(21)_2$. In this case, we have considered that the nonlinear parameter ε has the value of 50. Notice that the numerical integration solutions of (21) are almost indistinguishable from those computed by using the equivalent transformation forms. Here the gray solid lines represent the numerical integration solutions of (21), while the blue dashed lines described the numerical integration solutions obtained from the equivalent equations of motion. Therefore, we can conclude that our equivalent transformation approach provides accurate solutions to (21) if the form $(23)_1$ is used to derive the approximate solution of y_2.

Also notice from Table 4 that the smallest RMSE values, computed when the canonical form (7) of (19) is used to derive its equivalent representation form, are on $0 < \varepsilon \leq 0.25$, that is, when the equivalent form $(11)_1$ is substituted into $(7)_2$. Therefore, if one wants to have solutions that describe well the numerical integration solutions of (21), we need to use their canonical representation form at values of ε on the interval $0 < \varepsilon \leq 0.25$. For larger nonlinear system parameter values, good predictions of the original equation of motion are

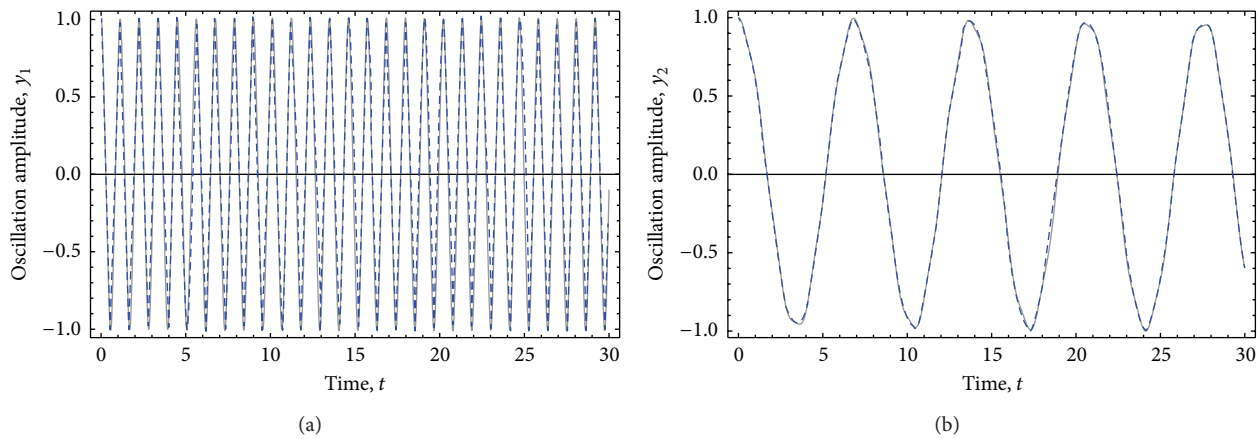

FIGURE 3: Amplitude-time response curves computed from the numerical integration solutions of (21) and those provided by substituting $(23)_1$ into $(21)_2$. The parameter values used to obtain these plots were $\beta = 1/5$ and $r_2 = 1$, $\varepsilon = 50$, with $\sigma_{10}(0) = 1$, $\dot{\sigma}(0) = 0$, $z_{10}(0) = -1$, $\dot{z}(0) = 0$, and $u_1 = -0.4$, $u_2 = 0.1$, $u_3 = -0.01$, and $u_4 = -0.315$. Here, the gray solid lines describe the numerical integration solutions of (21), while the blue dashed lines represent the numerical solutions obtained from the derived equivalent nonlinear equations of motion. In this case, the computed RMSE values were 0.1006, for y_1, and 0.0102, for y_2.

obtained when the equivalent form $(23)_1$ is substituted into $(21)_2$.

2.3. Example 3: A System with Three Nonlinear Springs. We now derive the equivalent representation form of two-mass system with three nonlinear springs introduced in [17] and whose differential equation of motion is given by

$$\begin{Bmatrix} m & 0 \\ 0 & m \end{Bmatrix} \begin{bmatrix} \ddot{x}_1 \\ \ddot{x}_2 \end{bmatrix} + \begin{Bmatrix} k_1 + k_2 & -k_2 \\ -k_2 & k_1 + k_2 \end{Bmatrix} \begin{bmatrix} x_1 \\ x_2 \end{bmatrix} + \begin{Bmatrix} k_3 (x_1 - x_2)^3 + \varepsilon k_4 x_1^3 \\ k_3 (x_2 - x_1)^3 + \varepsilon k_4 x_2^3 \end{Bmatrix} = 0, \tag{25}$$

with initial conditions $x_1(0) = x_{10}$, $\dot{x}_1(0) = 0$, $x_2(0) = x_{20}$, and $\dot{x}_2(0) = 0$. If we introduce the transformations $x_1 = (y_1 + y_0)/2$ and $x_2 = (y_0 - y_1)/2$, thus (25) can be written as

$$\begin{Bmatrix} \ddot{y}_0 \\ \ddot{y}_1 \end{Bmatrix} + \begin{Bmatrix} \omega_{n1}^2 & 0 \\ 0 & \omega_{n2}^2 \end{Bmatrix} \begin{bmatrix} y_0 \\ y_1 \end{bmatrix} + \begin{Bmatrix} \dfrac{\varepsilon k_4}{(4m)\, y_0^3} + \dfrac{\varepsilon k_4}{(4m)\, y_0 y_1^2} \\ \dfrac{\varepsilon k_4}{(4m)\, y_0^2 y_1} + \left(\dfrac{\beta + \varepsilon k_4}{(4m)} \right) y_1^3 \end{Bmatrix} = 0, \tag{26}$$

with initial conditions given as $y_0(0) = y_{00}$, $\dot{y}_0(0) = \dot{y}_{00}$, $y_1(0) = y_{10}$, and $\dot{y}_1(0) = \dot{y}_{10}$. Notice that (26) has the same form of (7) with system parameters given as

$$\omega_{n1}^2 = \frac{k_1}{m}, \qquad \omega_{n2}^2 = \frac{k_1 + 2k_2}{m}, \qquad \varphi_1 = \varphi_3 = \frac{\varepsilon k_4}{(4m)},$$
$$\varphi_2 = \varphi_4 = 0, \qquad \varphi_6 = \frac{\varepsilon k_4}{(4m)}, \tag{27}$$
$$\varphi_8 = \beta + \frac{\varepsilon k_4}{4m}, \qquad \varphi_5 = \varphi_7 = 0, \qquad \beta = \frac{2k_3}{m}.$$

Therefore and in accordance with our transformation approach, (26) are transformed into (11) in which

$$b_1 = \frac{\varphi_3 \nu_2^2 + 3\omega_{n1}^2}{3}; \qquad b_2 = \varphi_1;$$
$$b_3 = \frac{\varphi_6 \nu_{11}^2 + 3\omega_{n2}^2}{3}; \qquad b_4 = \varphi_8. \tag{28}$$

To assess the accuracy of the equivalent equations of motion when compared to the original ones (25), let us consider the parameter values of $k_1 = k_2 = k_3 = k_4 = 1$, $m = 1$, and $\varepsilon = -2.9$ and initial conditions $y_0(0) = 0.5$, $\dot{y}_0(0) = 0$, $y_1(0) = 1.5$, and $\dot{y}_1(0) = 0$. Figure 4 shows the amplitude-time response curves obtained by numerical integration of the corresponding equations of motion by using the Runge-Kutta method. One can notice from Figure 4 that the amplitude-time response curves obtained from (11) provide periodic solutions that cannot capture the high frequency components exhibited by the numerical amplitude-time curves plotted from (25). However, if we substitute the exact solution of $(11)_1$ into $(7)_2$ and plot its corresponding numerical integration solution, the high frequency components are captured as illustrated in Figure 5. Therefore, we can conclude that if during the dynamic analysis processes the motion of the coordinate y_1 exhibits harmonic behavior at lower angular frequency values, then the dynamics response behavior of this coordinate solution can be used to obtain the high frequency components exhibited by the remaining coordinate. In fact and for the nonlinear parameter value of $\varepsilon = -2.9$, the RMSE values, for the time interval shown in Figure 5, do not exceed 0.3159 and 0.1792 for y_0 and y_1, respectively.

We next increase the system nonlinearity at the value of $\varepsilon = -3.1$ and plot the corresponding amplitude versus time response curves. Notice from Figure 6 that when $t \geq 4$, the numerical integration solution of the equations of motion (25) obtained by using the Runge-Kutta numerical method fails in spite of using the several solver options provided by

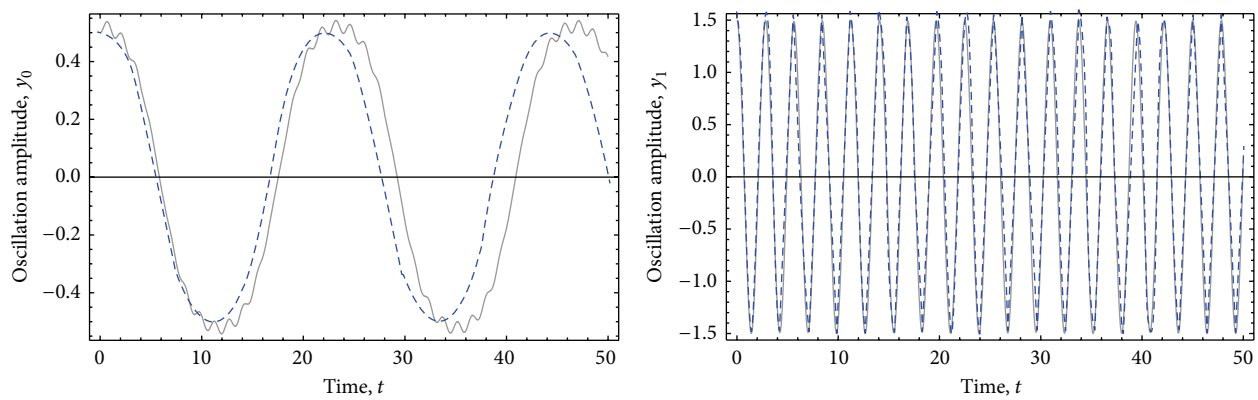

(a) (b)

Figure 4: Amplitude-time response curves computed from the numerical integration solutions of (26) and those provided by (11). The parameter values used to obtain these plots were $m = 1$, $k_1 = k_2 = k_3 = k_4 = 1$, and $\varepsilon = -2.9$, with $y_0(0) = 0.5$, $\dot{y}_0(0) = 0$, $y_1(0) = 1$, $\dot{y}_1(0) = 0$, $\nu_{11} = 1.1935$, and $\nu_2 = 1.1935$. Here, the gray solid lines describe the numerical integration solutions of (26), while the blue dashed lines represent the numerical solutions obtained from the derived equivalent nonlinear equations of motion. In this case, the computed RMSE values were 0.3159, for y_0, and 0.0358, for y_1.

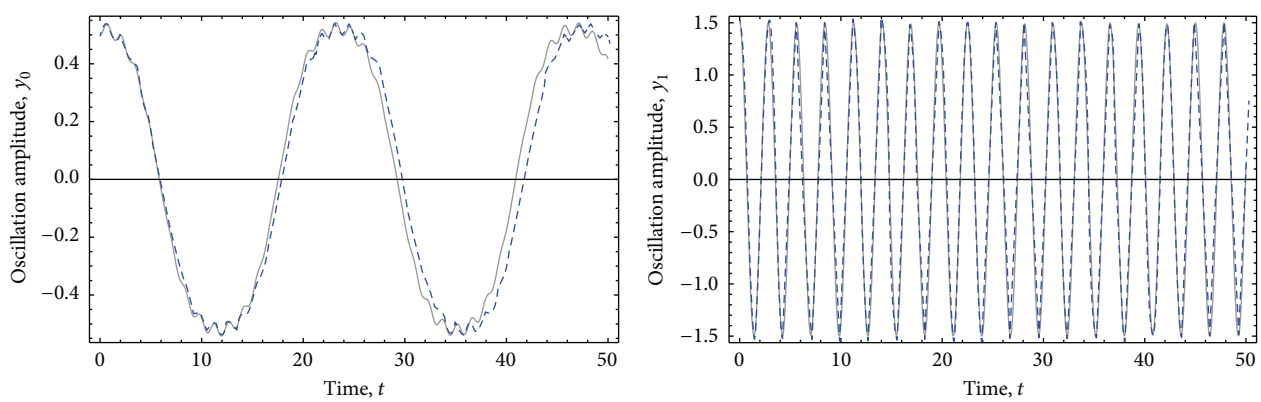

(a) (b)

Figure 5: Amplitude-time response curves computed from the numerical integration solutions of (26) and those provided by substituting $(11)_1$ into $(7)_2$. The parameter values used to obtain these plots were $m = 1$, $k_1 = k_2 = k_3 = k_4 = 1$, and $\varepsilon = -2.9$, with $y_0(0) = 0.5$, $\dot{y}_0(0) = 0$, $y_1(0) = 1$, $\dot{y}_1(0) = 0$, $\nu_{11} = 1.1935$, and $\nu_2 = 1.1935$. Here, the gray solid lines describe the numerical integration solutions of (26), while the blue dashed lines represent the numerical solutions obtained from the derived equivalent nonlinear equations of motion. In this case, the computed RMSE values were 0.3159, for y_0, and 0.1792, for y_1.

Mathematica 9.0 or the MATLAB V.2012a computer packages. In an attempt to capture the dynamics system response with this nonlinear value, we have numerically solved (25) by using the Enhanced Multistage homotopy perturbation method (EMHPM) introduced in [18]. This technique also fails at values of $t \geq 4$, as illustrated in Figure 6 by the black and the purple dots. However, the predicted amplitude versus time response curves computed by substituting $(11)_2$ into $(7)_1$ exhibits periodic behavior for the time interval shown in Figure 6. We can conclude that this transformation approach can help to obtain the numerical integration solutions of nonlinear dynamics systems in which the numerical integrations of the original equations of motion could fail because of the convergence of the corresponding numerical method.

2.4. Example 4: Finite Extensibility Nonlinear Elastic Absorber. We now focus our attention on finding the approximate solution of a finite extensibility nonlinear elastic (FENE) absorber attached to a nonlinear primary system [19], whose equations of motions are of the form

$$\begin{Bmatrix} m_1 & 0 \\ 0 & m_2 \end{Bmatrix} \begin{bmatrix} \ddot{x}_1 \\ \ddot{x}_2 \end{bmatrix} + \begin{Bmatrix} k_1 & 0 \\ 0 & 0 \end{Bmatrix} \begin{bmatrix} x_1 \\ x_2 \end{bmatrix} + \begin{Bmatrix} F_1(x_1, x_2) \\ F_2(x_1, x_2) \end{Bmatrix} = 0, \tag{29}$$

and the nonlinear restoring forces are given by

$$F_1(x_1, x_2) = \varepsilon x_1^3 - k_f \frac{(x_2 - x_1)}{1 - ((x_2 - x_1)/x_0)^2},$$
$$F_2(x_1, x_2) = k_f \frac{(x_2 - x_1)}{1 - ((x_2 - x_1)/x_0)^2}, \tag{30}$$

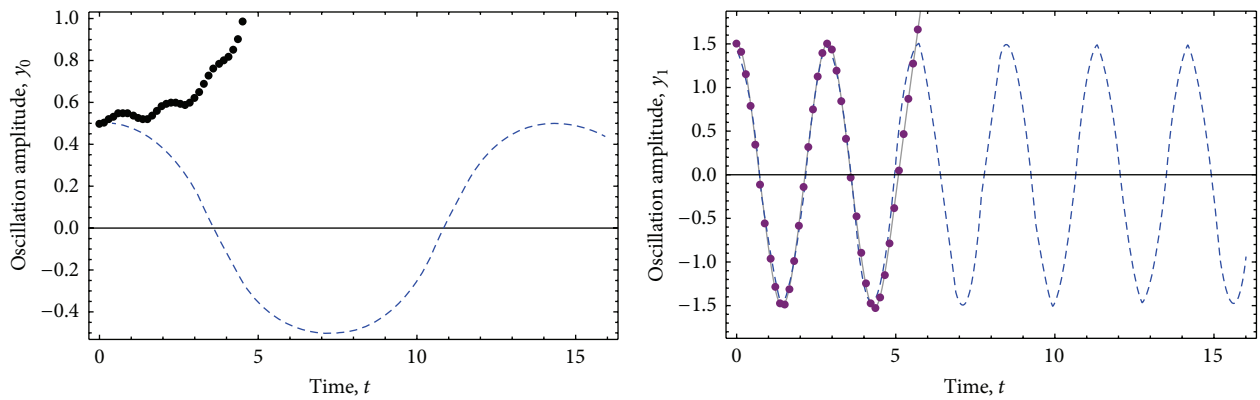

(a) (b)

Figure 6: Amplitude-time response curves computed from the numerical integration solutions of (26) and those provided by substituting $(11)_1$ into $(7)_2$. The parameter values used to obtain these plots were $m = 1$, $k_1 = k_2 = k_3 = k_4 = 1$, and $\varepsilon = -3.1$, with $y_0(0) = 0.5$, $\dot{y}_0(0) = 0$, $y_1(0) = 1$, $\dot{y}_1(0) = 0$, $\nu_{11} = 1.1935$, and $\nu_2 = 1.1935$. Here, the gray solid lines and the black and the purple dots describe the numerical integration solutions of (26) by using, respectively, the Runge-Kutta and the EMHPM methods, while the blue dashed lines representing the numerical solutions obtained from the derived equivalent nonlinear equations of motion.

with initial conditions $x_1(0) = x_{10}$, $\dot{x}_1(0) = 0$, $x_2(0) = x_{20}$, and $\dot{x}_2(0) = 0$. Here, m_1 is the mass of the primary system, m_2 represents the mass of the FENO system, k_1 and ε are, respectively, the linear and nonlinear stiffness parameters of the main system, and k_f and x_0 represent the coupling stiffness and the maximum possible extension of the FENO system, respectively. By introducing the transformations $y_1 = x_1/x_{10}$ and $y_2 = x_2/x_{20}$ into (29), we get that

$$\begin{Bmatrix} \ddot{y}_1 \\ \ddot{y}_2 \end{Bmatrix} + \begin{Bmatrix} \omega_{n1}^2 & 0 \\ 0 & 0 \end{Bmatrix} \begin{bmatrix} y_1 \\ y_2 \end{bmatrix} + \begin{Bmatrix} \varphi_1 x_1^3 - \varphi_2 \dfrac{A(y_2 - y_1 x_{10}/x_{20})}{1 - A^2(y_2 - y_1 x_{10}/x_{20})^2} \\ \varphi_3 \dfrac{A(y_2 - y_1 x_{10}/x_{20})}{1 - A^2(y_2 - y_1 x_{10}/x_{20})^2} \end{Bmatrix} = 0, \tag{31}$$

with initial conditions given as $y_1(0) = 1$, $\dot{y}_1(0) = 0$, $y_2(0) = 1$, and $\dot{y}_2(0) = 0$, and $A = x_{20}/x_0$, $\varphi_1 = \varepsilon x_{10}^2/m_1$, $\varphi_2 = k_f x_0/(m_1 x_{10} x_0)$, and $\varphi_3 = k_f x_0/(m_2 x_{20})$. We next use the Chebyshev polynomials of the first kind [9, 11] to derive the cubic-like representation form of the nonlinear rational restoring force of (31). This procedure yields

$$\begin{aligned} F(y) &= \frac{A(y_2 - y_1 x_{10}/x_{20})}{1 - A^2(y_2 - y_1 x_{10}/x_{20})^2} = \frac{Ay}{1 - A^2 y^2} \\ &= (b_1 - 3b_3)\, y + 4b_3 y^3, \end{aligned} \tag{32}$$

where $y = (y_2 - y_1 x_{10}/x_{20})$, and by definition

$$b_{2n+1}(A) = \frac{2}{\pi} \int_{-1}^{1} \left(1 - y^2\right)^{-1/2} F(y)\, T_{2n+1}(y)\, dy, \tag{33}$$

and T_{2n-1} are the Chebyshev polynomials of the first kind defined as

$$\begin{aligned} T_{2n+1}(x) &= \cos\left[(2n+1)\cos^{-1}(x)\right], \\ x &\in [-1, 1], \quad n = 0, 1, 2, \ldots. \end{aligned} \tag{34}$$

By using (33), we obtain that

$$\begin{aligned} b_1 &= \frac{2}{A}\left(\frac{1}{\sqrt{1 - A^2}} - 1\right), \\ b_3 &= \frac{2}{A^3}\left(\frac{4}{\sqrt{1 - A^2}} + A^2\left(1 - \frac{3}{\sqrt{1 - A^2}}\right) - 4\right). \end{aligned} \tag{35}$$

Thus, the FENO nonlinear restoring force $F(y)$ can be written in equivalent form as

$$F(y) \equiv \alpha y + \beta y^3, \tag{36}$$

in which

$$\begin{aligned} \alpha &= \frac{1}{A}\left\{2\left(\frac{1}{\sqrt{1 - A^2}} - 1\right) - \frac{6}{A^2}\left(\frac{4}{\sqrt{1 - A^2}} + A^2\left(1 - \frac{3}{\sqrt{1 - A^2}}\right) - 4\right)\right\}, \\ \beta &= \frac{8}{A^3}\left\{\frac{4}{\sqrt{1 - A^2}} + A^2\left(1 - \frac{3}{\sqrt{1 - A^2}}\right) - 4\right\}. \end{aligned} \tag{37}$$

Based on (37), it is clear that the equivalent representation form (36) of the restoring force (32) holds if and only if $x_{20} < x_0$. Thus, (31) can be written as

$$\begin{Bmatrix} \ddot{y}_1 \\ \ddot{y}_2 \end{Bmatrix} + \begin{Bmatrix} \omega_{n1}^2 & 0 \\ 0 & 0 \end{Bmatrix} \begin{bmatrix} y_1 \\ y_2 \end{bmatrix} + \begin{Bmatrix} \varphi_1 x_1^3 - \varphi_2 \left\{ \alpha \left(y_2 - \dfrac{y_1 x_{10}}{x_{20}} \right) + \beta \left(y_2 - \dfrac{y_1 x_{10}}{x_{20}} \right)^3 \right\} \\ \varphi_3 \left\{ \alpha \left(y_2 - \dfrac{y_1 x_{10}}{x_{20}} \right) + \beta \left(y_2 - \dfrac{y_1 x_{10}}{x_{20}} \right)^3 \right\} \end{Bmatrix} = 0. \tag{38}$$

We next apply the aforementioned nonlinear transformation approach to (38), to obtain that

$$\ddot{y}_1 + a_1 y_1 + a_2 y_1^3 = 0; \qquad \ddot{y}_2 + a_3 y_2 + a_4 y_2^3 = 0, \tag{39}$$

where the a_i are given as

$$\begin{aligned} a_1 &= \omega_{n1}^2 + \varphi_2 \left(2\alpha x_{20} \left(32 x_{10} u_1 - 45 x_{20} u_2 \right) + \beta \sigma_2 \left\{ 64 x_{10} x_{20} u_1 u_2 - 30 x_{10}^2 u_1^2 - 45 x_{20}^2 u_2^2 \right\} \right) \frac{1}{64 x_{20}^2 u_1}, \\ a_2 &= \varphi_1 + \varphi_2 \times \left(70 \alpha x_{20}^3 u_2 + \beta \left(64 x_{10}^3 u_1^3 - 70 x_{10}^2 x_{20} u_1^2 u_2 + 35 x_{20}^3 u_2^3 \right) \right) \times \frac{1}{64 x_{20}^3 u_1^3}, \\ a_3 &= \frac{\varphi_3}{64 x_{20}^3 u_{22}} \times \left(\alpha \left(-90 x_{10} x_{20} u_{11} + 64 x_{20}^3 u_{22} \right) + \beta x_{10} u_{11} \times \left(-45 x_{10}^2 u_{11}^2 + 64 x_{10} x_{20} u_{11} u_{22} - 30 x_{20}^2 u_{22}^2 \right) \right), \\ a_4 &= \frac{\varphi_3}{64} \times \left(64\beta + \frac{35 \left(2\alpha x_{10} x_{20} u_{11} + \beta x_{10}^3 u_{11}^3 \right)}{x_{20}^3 u_{22}^3} - \frac{70 \beta x_{10} u_{11}}{x_{20} u_{22}} \right). \end{aligned} \tag{40}$$

To assess the degree of accuracy attaining by (39), let us consider the parameter values of $m_1 = 1$, $m_2 = 1/2$, $k_1 = 1$, $k_f = 1$, $x_0 = 1$, and $\varepsilon = 1$, with $x_0(0) = 1/2$, $\dot{x}_0(0) = 0$, $x_1(0) = 0.99$, and $\dot{x}_1(0) = 0$. Figure 7 shows the amplitude-time response curves of (31) compared to those obtained by substituting $(39)_1$ into $(38)_2$. Here, the computed parameter values are $\alpha = -15.4771$, $\beta = 37.0369$, $a_1 = 0.3305$, $a_2 = 0.5512$, $a_3 = -107.549$, and $a_4 = 96.7734$, with $u_1 = -1.991$, $u_2 = -1.115$, $u_{11} = -0.7$, and $u_{22} = -4.6$. In this case, the computed RMSE values for y_1 and y_2 were, respectively, 0.1965 and 0.2443. Table 5 shows the RMSE computed at different values of x_{20}. Notice that when x_{20} tends to x_0, the RMSE values tend in general, to decrease, while the global error exhibits a linear increasing behavior, as illustrated in Figure 8.

2.5. Example 5: A Two-Degree-of-Freedom System with Irrational Restoring Force. As a final example, let us consider the system shown in Figure 9 having two masses, m_1 and m_2 which are connected by four elastic springs of stiffness k_1 and k_2 having an undeformed length, l_0. Furthermore, the element with mass m_1 is moving on a smooth horizontal bearing surface whose motion is restricted by an elastic linear spring of stiffness k_3. By using Newton second law, it is easy to show that the equations of motion are

$$\begin{Bmatrix} 1 & 0 \\ 0 & 1 \end{Bmatrix} \begin{bmatrix} \ddot{x}_1 \\ \ddot{x}_2 \end{bmatrix} + \begin{Bmatrix} \dfrac{k_3}{m_1} & 0 \\ 0 & 0 \end{Bmatrix} \begin{bmatrix} x_1 \\ x_2 \end{bmatrix} + \begin{Bmatrix} -\dfrac{2k_1}{m_1} + B & 0 \\ 0 & \dfrac{2k_1}{m_2} + B_1 \end{Bmatrix} \begin{bmatrix} (x_2 - x_1) \\ (x_2 - x_1) \end{bmatrix} + \begin{Bmatrix} F_1(x_1, x_2) \\ F_2(x_1, x_2) \end{Bmatrix} = 0, \tag{41}$$

where the irrational restoring forces are given by

$$\begin{aligned} F_1(x_1, x_2) &= \frac{C(x_2 - x_1)}{\sqrt{1 + A^2 (x_2 - x_1)^2}}, \\ F_2(x_1, x_2) &= \frac{C_1(x_2 - x_1)}{\sqrt{1 + A^2 (x_2 - x_1)^2}}. \end{aligned} \tag{42}$$

Here $B = -2k_2/m_1$, $B_1 = 2k_2/m_2$, $C = 2k_2/m_1$, and $C_1 = -2k_2/m_2$. The system (41) can be cast in different form by setting $x_1 = (w_1 - w_2)/2$ and $x_2 = (w_2 + w_1)/2$, and after some algebraic manipulations, we get that

$$\begin{Bmatrix} 1 & 0 \\ 0 & 1 \end{Bmatrix} \begin{bmatrix} \ddot{w}_1 \\ \ddot{w}_2 \end{bmatrix} + \begin{Bmatrix} \dfrac{k_3}{(2m_1)} & k_{11} \\ k_{22} & -\dfrac{k_3}{(2m_1)} \end{Bmatrix} \begin{bmatrix} w_1 \\ w_2 \end{bmatrix} + \begin{Bmatrix} \dfrac{w_2 (C + C_1)}{2\sqrt{1 + A^2 w_2^2}} \\ -\dfrac{w_2 (C_1 - C)}{2\sqrt{1 + A^2 w_2^2}} \end{Bmatrix} = 0, \tag{43}$$

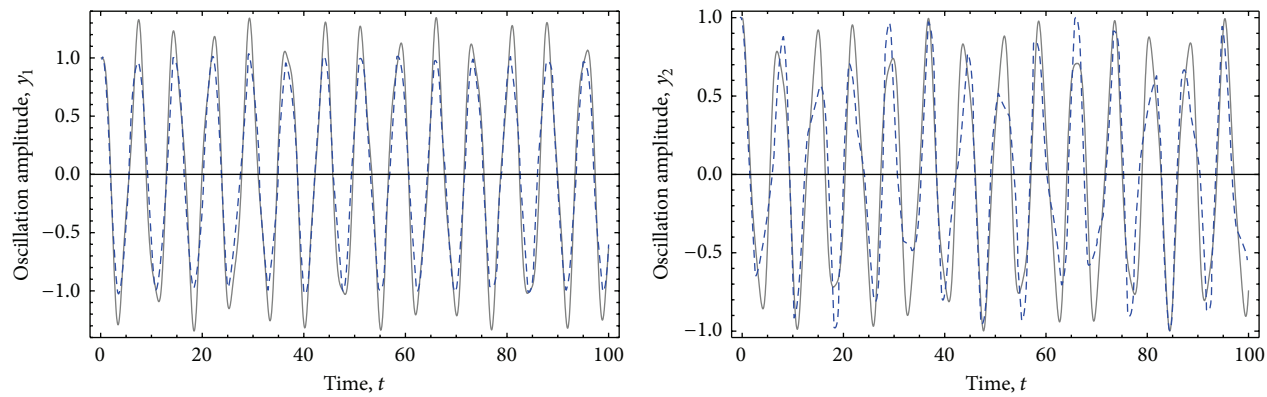

(a) (b)

FIGURE 7: Amplitude-time response curves computed from the numerical integration solutions of (31) and those provided by substituting $(39)_1$ into $(38)_2$. The parameter values used to obtain these plots were $m_1 = 1$, $m_2 = 1/2$, $k_1 = 1$, $k_f = 1$, $x_0 = 1$, and $\varepsilon = 1$, with $x_0(0) = 1/2$, $\dot{x}_0(0) = 0$, $x_1(0) = 0.99$, $\dot{x}_1(0) = 0$, $u_1 = -1.991$, $u_2 = -1.115$, $u_{11} = -0.7$, and $u_{22} = -4.6$. Here, the gray solid lines describe the numerical integration solutions of (31), while the blue dashed lines represent the numerical solutions obtained from the derived equivalent nonlinear equations of motion.

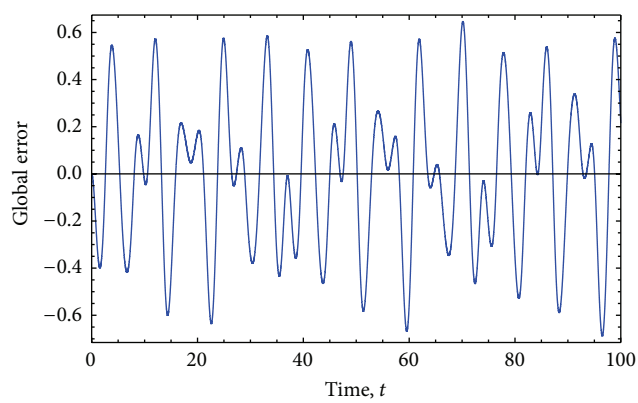

FIGURE 8: Global error behavior plotted versus time.

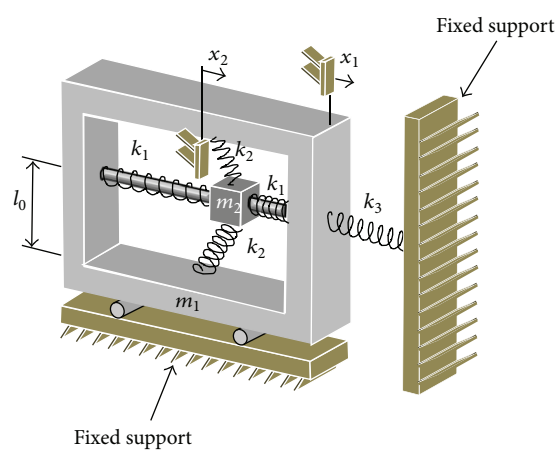

FIGURE 9: Schematic of a two-degree-of-freedom system with irrational restoring force.

with initial conditions $w_1(0) = w_{10}$, $\dot{w}_1(0) = 0$, $w_2(0) = w_{20}$, and $\dot{w}_2(0) = 0$. If we set $z_1 = w_1/w_{10}$ and $z_2 = w_2/w_{20}$, then (43) becomes

$$\begin{Bmatrix} 1 & 0 \\ 0 & 1 \end{Bmatrix} \begin{bmatrix} \ddot{z}_1 \\ \ddot{z}_2 \end{bmatrix} + \begin{Bmatrix} \dfrac{k_3}{(2m_1)} & \dfrac{k_{11} w_{20}}{w_{10}} \\ k_{22} & -\dfrac{k_3 w_{10}}{(2m_1 w_{20})} \end{Bmatrix} \begin{bmatrix} z_1 \\ z_2 \end{bmatrix} + \begin{Bmatrix} \dfrac{z_1 (C + C_1) w_{20}}{w_{10}\sqrt{1 + A^2 w_2^2 w_{20}^2}} \\ -\dfrac{z_1 (C_1 - C) w_{20}}{w_{10}\sqrt{1 + A^2 w_2^2 w_{20}^2}} \end{Bmatrix} = 0, \tag{44}$$

where

$$k_{11} = \frac{1}{2}\left(-\frac{k_3/2 + 2k_1}{m_1} + \frac{2k_1}{m_2} + B + B_1\right), \qquad k_{22} = \frac{1}{2}\left(\frac{k_3/2 + 2k_1}{m_1} + \frac{2k_1}{m_2} + B_1 - B\right), \tag{45}$$

with $z_1(0) = 1$, $\dot{z}_1(0) = 0$, $\dot{z}_2(0) = 1$, and $z_2(0) = 0$. By using the Chebyshev polynomials of the first kind, the cubic-like representation form of the irrational restoring force becomes

$$\frac{z_1}{\sqrt{1 + A_1^2 w_2^2 w_{20}^2}} \equiv \alpha z_1 + \beta z_1^3, \tag{46}$$

where

$$\alpha = \frac{4}{\pi A^2}\left\{E\left(-A^2\right) - K\left(-A^2\right) - \frac{1}{A^2} \times \left(\left(8+5A^2\right)K\left(-A^2\right) - \left(8+A^2\right)E\left(-A^2\right)\right)\right\},$$

$$\beta = \frac{16}{3\pi A^4} \times \left\{\left(8+5A^2\right)K\left(-A^2\right) - \left(8+A^2\right)E\left(-A^2\right)\right\}. \tag{47}$$

Here $K(-A^2)$ and $E(-A^2)$ are the complete elliptic integral of the first and second kind for the modulus A, respectively. Thus, (44) can be rewritten as

$$\begin{Bmatrix} 1 & 0 \\ 0 & 1 \end{Bmatrix}\begin{bmatrix} \ddot{z}_1 \\ \ddot{z}_2 \end{bmatrix} + \begin{Bmatrix} \dfrac{k_3}{(2m_1)} & \dfrac{k_{11}w_{20}}{w_{10}} \\ k_{22} & -\dfrac{k_3 w_{10}}{(2m_1 w_{20})} \end{Bmatrix}\begin{bmatrix} z_1 \\ z_2 \end{bmatrix} + \begin{Bmatrix} \dfrac{(C+C_1)\,w_{20}\left\{\alpha z_1 + \beta z_1^3\right\}}{w_{10}} \\ -(C_1 - C)\left\{\alpha z_1 + \beta z_1^3\right\} w_{20}/w_{10} \end{Bmatrix} = 0. \tag{48}$$

Application of the proposed nonlinear transformation approach to (48) yields

$$\ddot{z}_1 + a_1 z_1 + a_2 z_1^3 = 0; \qquad \ddot{z}_2 + a_3 z_2 + a_4 z_2^3 = 0, \tag{49}$$

where the a_i are given as

$$\begin{aligned} a_1 &= \frac{1}{64 m_1 w_{10} u_1}\left(32 k_3 w_{10} u_1 + 90\alpha m_1 w_{10} u_2 + 90 k_{11} m_1 w_{20} u_2 + 45\beta m_1 w_{10} u_2^3\right), \\ a_2 &= -\frac{35}{64 m_1 w_{10} u_1^3}\left(2\alpha w_{10} u_2 + 2k_{11} w_{20} u_2 + \beta w_{10} u_2^3\right), \\ a_3 &= -\frac{45 k_3 w_{10} u_{11} - 64\alpha m_1 w_{20} u_{22} - 64 k_{22} m_1 w_{20} u_{22}}{64 m_1 w_{20} u_{22}^3}, \\ a_4 &= -\frac{-35 k_3 w_{10} u_{11} - 64\beta m_1 w_{20} u_{22}^3}{64 m_1 w_{20} u_{22}^3}. \end{aligned} \tag{50}$$

Figure 10 illustrates the numerical predictions obtained by substituting $(49)_1$ into $(48)_2$, as well as those computed from the numerical integration solution of (48). In Example 5, we have used the following system parameter values: $m_1 = 1$, $m_2 = 1/2$, $k_1 = 1$, $k_2 = 1$, $k_3 = 1$, and $A = 1$, with initial conditions given as $w_1(0) = 4$, $\dot{w}_1(0) = 0$, $w_2(0) = 2$, and $\dot{w}_2(0) = 0$. The predicted parameter values are $\alpha = 4.7082$, $\beta = -2.1374$, $a_1 = -0.5442$, $a_2 = 1.7564$, $a_3 = 8.5590$, and $a_4 = 0.1652$, with $u_1 = -0.68$, $u_2 = 0.5$, $u_{11} = -0.3$, and $u_{22} = 0.55$. Notice from Figure 10 that our numerical integration predictions computed from $(49)_1$ and $(48)_2$ follow the amplitude-time response curves computed from (48) with RMSE values of 0.2095 for z_1 and 0.1318 for z_2, respectively. The system global error as illustrated in Figure 11 tends to linearly grow as time increases. Of course, other values of the system initial conditions can be used to study the quantitative and qualitative system dynamics response; however, when the system parameter changes, it could be necessary to adjust the values of u_i and u_{ii} in order to satisfy (8).

Table 5: RMSE values computed by using the equivalent representation form of (31) with $u_1 = -1.991$, $u_2 = -1.115$, $u_{11} = -0.7$, and $u_{22} = -4.6$.

x_{20}	RMSE $y_1(x)$	RMSE $y_2(x)$
0.75	0.9981	1.1200
0.80	1.0245	1.0467
0.85	1.0330	0.9560
0.90	0.5851	0.5029
0.95	1.0122	0.8019
0.99	0.1965	0.2443

3. Conclusions

We have introduced a nonlinear transformation approach to determine the equivalent representation form of two degree-of-freedom oscillatory systems with nonlinear restoring forces. It has been shown that this nonlinear transformation approach decoupled the system equation into two Duffing equations. It has been found that the numerical integration of the equivalent equations of motion, of the five dynamic systems examined here, follows well the computed numerical values obtained from the original equations of motion. Furthermore, it has been shown that by substituting the decouple equation related to the $x_1(y_1)$ coordinate system into the original equation of motion described by $x_2(y_2)$, it provides the lower RMSE values. However, when the canonical representation form of the original equations of motion is used to decouple the corresponding equations, the smallest RMSE values were found at small values of the nonlinear parameter ε.

We also have found in Example 3 that our equivalent representation form can capture high frequency system components if the exact solution of the cubic-like representation form of the coordinate y_1 is used to find the dynamics response of the y_0 coordinate. Besides, the corresponding equivalent equations of motion can be numerically integrated at the value of $\varepsilon = -3.1$ while the numerical integration solution of the original equations of motion (25), by using the Runge-Kutta, fails in spite of using the several solver options provided by Mathematica 9.0 or the MATLAB V.2012a computer packages. We next applied the EMHPM to find the numerical solution of (25) but it was found that this technique provides numerical results that diverge when $t \geq 4$. However, the numerical integration of our equivalent representation form provides solutions that describe the system dynamics periodic behavior.

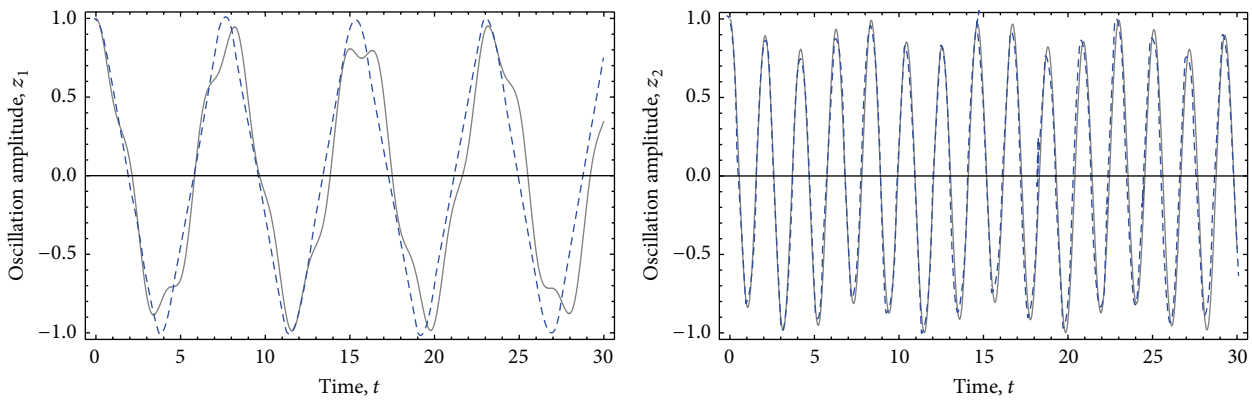

(a) (b)

Figure 10: Amplitude-time response curves computed from the numerical integration solutions of (48) and those provided by substituting $(49)_1$ into $(48)_2$. The parameter values used to obtain these plots were $m_1 = 1$, $m_2 = 1/2$, $k_1 = 1$, $k_2 = 1$, $k_3 = 1$, $A = 1$, $w_1(0) = 4$, $\dot{w}_1(0) = 0$, $w_2(0) = 2$, $\dot{w}_2(0) = 0$, $\alpha = 4.7082$, $\beta = -2.1374$, $a_1 = -0.5442$, $a_2 = 1.7564$, $a_3 = 8.5590$, and $a_4 = 0.1652$, with $u_1 = -0.68$, $u_2 = 0.5$, $u_{11} = -0.3$, and $u_{22} = 0.55$. Here, the gray solid lines describe the numerical integration solutions of (31), while the blue dashed lines represent the numerical solutions obtained from the derived equivalent nonlinear equations of motion.

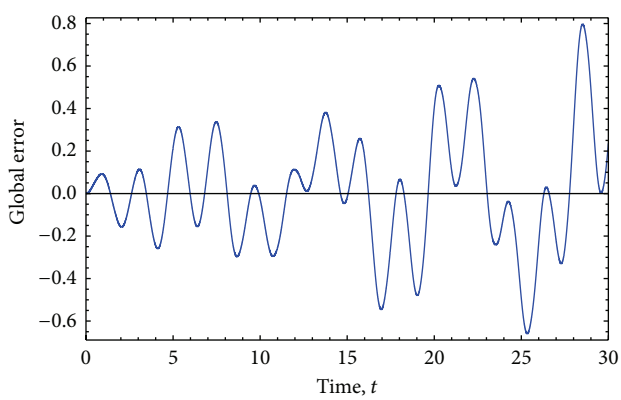

Figure 11

In the case of Examples 4 and 5, we believe that the RMSE and the global error magnitudes are mainly due to two factors: (a) the Chebyshev polynomial representation of the system restoring forces and (b) the equivalent representation form of the original equations of motion that are based on cubic-like Duffing's equations. These two factors affect the accuracy achieved during the solution process; however, the quantitative and qualitative system response are captured with good degree of accuracy.

Therefore, it can be concluded, in accordance with some of the systems studied here, that if one wants to have the smallest RMSE values when using the proposed nonlinear transformation approach, the canonical representation form has to be used for weak nonlinear system; however, for larger values of ε, the accurate results are obtained when the original equations of motion were decoupled. Based on the numerical simulation results, it is clear that our method is a promising technique that could provide equivalent representation forms of dynamic systems with two or more degrees of freedom that can follow the numerical integration solutions of the original equations of motion, at larger nonlinear parameter values.

Conflict of Interests

The authors declare that there is no conflict of interests regarding the publication of this paper.

Acknowledgments

This work was funded by Tecnológico de Monterrey-Campus Monterrey, through the Research Chair in Nanomaterials for Medical Devices and the Research Chair in Intelligent Machines. Additional support was provided from the European Commission Project, IREBID (FP7-PEOPLE-2009-IRSES-247476), and from Consejo Nacional de Ciencia y Tecnología (Conacyt), México.

References

[1] A. Elías-Zúñiga and O. Martínez-Romero, "Accurate solutions of conservative nonlinear oscillators by the enhanced cubication method," *Mathematical Problems in Engineering*, vol. 2013, Article ID 842423, 9 pages, 2013.

[2] A. Elías-Zúñiga and O. Martínez-Romero, "Investigation of the equivalent representation form of damped strongly nonlinear oscillators by a nonlinear transformation approach," *Journal of Applied Mathematics*, vol. 2013, Article ID 245092, 7 pages, 2013.

[3] R. Bhattacharyya, P. Jain, and A. Nair, "Normal mode localization for a two degrees-of-freedom system with quadratic and cubic non-linearities," *Journal of Sound and Vibration*, vol. 249, no. 5, pp. 909–919, 2002.

[4] C. Touzé, O. Thomas, and A. Chaigne, "Hardening/softening behaviour in non-linear oscillations of structural systems using non-linear normal modes," *Journal of Sound and Vibration*, vol. 273, no. 1-2, pp. 77–101, 2004.

[5] N. A. Alexander and F. Schilder, "Exploring the performance of a nonlinear tuned mass damper," *Journal of Sound and Vibration*, vol. 319, no. 1-2, pp. 445–462, 2009.

[6] T. Pirbodaghi and S. Hoseini, "Nonlinear free vibration of a symmetrically conservative two-mass system with cubic nonlinearity," *Journal of Computational and Nonlinear Dynamics*, vol. 5, no. 1, Article ID 011006, 6 pages, 2010.

[7] J. Cai, X. Wu, and Y. P. Li, "An equivalent nonlinearization method for strongly nonlinear oscillations," *Mechanics Research Communications*, vol. 32, no. 5, pp. 553–560, 2005.

[8] A. F. Vakakis and R. H. Rand, "Normal modes and global dynamics of a two-degree-of-freedom non-linear system-II. High energies," *International Journal of Non-Linear Mechanics*, vol. 27, no. 5, pp. 875–888, 1992.

[9] A. Beléndez, M. L. Alvarez, E. Fernández, and I. Pascual, "Cubication of conservative nonlinear oscillators," *European Journal of Physics*, vol. 30, pp. 973–981, 2009.

[10] A. Beléndez, D. I. Méndez, E. Fernández, S. Marini, and I. Pascual, "An explicit approximate solution to the Duffing-harmonic oscillator by a cubication method," *Physics Letters A*, vol. 373, no. 32, pp. 2805–2809, 2009.

[11] A. Beléndez, G. Bernabeu, J. Francés, D. I. Méndez, and S. Marini, "An accurate closed-form approximate solution for the quintic Duffing oscillator equation," *Mathematical and Computer Modelling*, vol. 52, no. 3-4, pp. 637–641, 2010.

[12] L. Meirovitch, *Elements of Vibration Analysis*, McGraw-Hill, New York, NY, USA, 1986.

[13] A. Elías-Zúñiga, "On the elliptic balance method," *Mathematics and Mechanics of Solids*, vol. 8, no. 3, pp. 263–279, 2003.

[14] M. P. Calvo and E. Hairer, "Accurate long-term integration of dynamical systems," *Applied Numerical Mathematics*, vol. 18, no. 1–3, pp. 95–105, 1995.

[15] M. Calvo, S. González-Pinto, and J. I. Montijano, "Global error estimation based on the tolerance proportionality for some adaptive Runge-Kutta codes," *Journal of Computational and Applied Mathematics*, vol. 218, no. 2, pp. 329–341, 2008.

[16] R. Weiner and G. Yu. Kulikov, "Local and global error estimation and control within explicit two-step peer triples," *Journal of Computational and Applied Mathematics*, vol. 262, pp. 261–270, 2013.

[17] L. Cveticanin, "Vibrations of a coupled two-degree-of-freedom system," *Journal of Sound and Vibration*, vol. 247, no. 2, pp. 279–292, 2001.

[18] D. Olvera, A. Elías-Zúñiga, H. Martínez-Alfaro, L. N. López de Lacalle, C. A. Rodríguez, and F. J. Campa, "Determination of the stability lobes in milling operations based on homotopy and simulated annealing techniques," *Mechatronics*, vol. 24, no. 3, pp. 177–185, 2014.

[19] M. Febbo and S. P. Machado, "Nonlinear dynamic vibration absorbers with a saturation," *Journal of Sound and Vibration*, vol. 332, pp. 1465–1483, 2013.

[20] Q. Cao and Y. Xiong, "Dynamic analysis of a two degree of freedom system with irrational nonlinearity," in *Proceedings of the European Nonlinear Oscillations Conference (ENOC '11)*, Rome, Italy, July 2011.